TU Delft

Delft University of Technology

Specific selectivity of simple oxides towards CH4 activation

Pinto, Donato; Urakawa, Atsushi

DOI
10.1016/j.cattod.2025.115337

Publication date
2025

Document Version
Final published version

Published in
Catalysis Today

Citation (APA)
Pinto, D., & Urakawa, A. (2025). Specific selectivity of simple oxides towards CH4 activation. *Catalysis Today*, *455*, Article 115337. https://doi.org/10.1016/j.cattod.2025.115337

Important note
To cite this publication, please use the final published version (if applicable).
Please check the document version above.

Copyright
Other than for strictly personal use, it is not permitted to download, forward or distribute the text or part of it, without the consent of the author(s) and/or copyright holder(s), unless the work is under an open content license such as Creative Commons.

Takedown policy
Please contact us and provide details if you believe this document breaches copyrights.
We will remove access to the work immediately and investigate your claim.

This work is downloaded from Delft University of Technology.
For technical reasons the number of authors shown on this cover page is limited to a maximum of 10.

Catalysis Today 455 (2025) 115337

Contents lists available at ScienceDirect

Catalysis Today

journal homepage: www.elsevier.com/locate/cattod

Specific selectivity of simple oxides towards CH_4 activation

Donato Pinto [a,b], Atsushi Urakawa [a,b,*]

[a] Institute of Chemical Research of Catalonia (ICIQ), The Barcelona Institute of Science and Technology, Av. Països Catalans 16, Tarragona 43007, Spain
[b] Catalysis Engineering, Department of Chemical Engineering, Delft University of Technology, Van der Maasweg 9, Delft 2629 Hz, Netherlands

ARTICLE INFO

Keywords:
Methane activation
Metal oxides
Oxidative coupling of methane
Syngas
Transient study

ABSTRACT

Simple metal oxides exhibit noticeable catalytic activity in methane conversion reactions. However, their catalytic role in the selective activation of CH_4 to more valuable products (CO, H_2, olefins) is often masked by the highly oxidative reaction conditions and by complex catalyst formulations. Transient studies of the direct interaction of CH_4 with simple catalytic systems, including rare-earth (La_2O_3, Nd_2O_3, Y_2O_3), alkali-earth (MgO) and reducible (TiO_2), reveal peculiar selectivity for different monometallic oxides. Rare-earth metal oxides show high initial activity towards partial oxidation products (CO, H_2), while MgO possesses unique selectivity towards coupling products (C_2H_6 and C_2H_4) with remarkable activity in dehydrogenation reactions. A continuous supply of lattice oxygen species for the selective oxidation of CH_4 to CO is provided by TiO_2, which can effectively prevent accumulation of C deposits. The results indicate the roles played by the metal oxide materials and provide a basis for rational design of catalysts and reaction conditions for the selective conversion of CH_4.

1. Introduction

As main component of the natural gas, methane represents a valid opportunity to substitute oil in the short-term as energy and chemical feedstock. Apart from energy generation, a major process for CH_4 utilisation is its reforming with H_2O to produce a valuable mixture of H_2 and CO (syngas). Syngas is an effective intermediate for additional chemical processes such as methanol synthesis or hydrocarbons production via Fischer-Tropsch synthesis [1]. Developing direct conversion of methane into value-added products would substantially reduce the energy and economic requirements of the indirect routes, however several challenges are associated with its selective conversion to chemicals [2–4]. From a thermodynamic point of view, methane is the most stable hydrocarbon in a wide temperature range (up to 1030 °C) [5]. The high stability of the molecule, and the deriving challenges to its activation, are related to the high symmetry of its tetrahedral structure, with equally spaced H atoms surrounding the C in the centre. In a radical reaction path, the first C-H bond breaking is necessary to activate the molecule and generate an active methyl radical. The high energy of the bond (439 kJ mol^{-1}) makes the activation highly endothermic, requiring extreme conditions to drive the reaction [4]. In homogeneous gas-phase reactions, C-C and C-H bond cleavage is observed only at very high temperatures (1200 °C) [5]. The use of strong oxidants can make the overall reaction exothermic, often at the cost of low selectivity, by the formation of undesired oxidation products as H_2O and CO_2. In order to lower the energetic requirements for methane activation and, at the same time, control the selectivity of the products, the employment of a catalyst is fundamental. Strong interaction with a catalyst surface reduces the symmetry of the molecule and facilitates the activation of the molecule by electron transfer [6].

With the promise of single-process conversion of CH_4 to olefins, and simultaneously cutting the process chain and its costs, the first oxidative coupling of methane (OCM) works were received with enthusiasm in the early 1980s [7]. Several works reported screening of simple oxides focusing the attention on their performance in OCM [8–10]. Alkaline-earth and rare-earth metal oxides often exhibited the best results, and there is a general agreement about the positive influence of the oxide basicity on the formation of coupling products [9,11]. However, a limit on the maximum C_2 products yield was found (< 30 %) [12], which inhibited the commercialisation of the process so far. Several attempts have been made to determine the mechanism in OCM reaction conditions [13,14]. It is generally agreed that the reaction starts with activation of CH_4 molecule by abstraction of a H atom by the catalyst and formation of a methyl radical ($\bullet CH_3$). Methyl radicals will then couple to form C_2H_6, and subsequent dehydrogenation yields C_2H_4. Alternatively, C_2 species can be further oxidised to undesired CO and CO_2 [4,15].

* Corresponding author at: Catalysis Engineering, Department of Chemical Engineering, Delft University of Technology, Van der Maasweg 9, Delft 2629 Hz, Netherlands.
E-mail addresses: d.pinto@tudelft.nl (D. Pinto), A.Urakawa@tudelft.nl (A. Urakawa).

https://doi.org/10.1016/j.cattod.2025.115337
Received 13 January 2025; Received in revised form 3 April 2025; Accepted 10 April 2025
Available online 11 April 2025
0920-5861/© 2025 The Author(s). Published by Elsevier B.V. This is an open access article under the CC BY license (http://creativecommons.org/licenses/by/4.0/).

However, in terms of identifying the catalytically active sites and establishing the nature of the C_2 selectivity on simple metal oxide catalysts, the information retrieved at those conditions are often inconclusive.

Understanding the mechanism of methane activation in highly oxidative conditions is complicated by the presence of highly reactive oxidant species (molecular oxygen, peroxide ion, superoxide radical, hydroxyl radicals) [16,17] that can react further leading to nonselective exothermic pathways, often associated with temperature and concentration gradients in the catalytic bed. On the contrary, unsteady-state operation permits to intrinsically separate the reducing and oxidising feeds, inhibiting the development of highly exothermic and unselective total oxidation pathways and highlighting the specific role and selectivity of the catalytically active sites [18–20]. In a previous contribution, we reported the contrast between similar performances of La_2O_3 and MgO towards CH_4 oxidative coupling and their substantial different activity in transient catalytic studies. These insights confirmed that the development of undesired temperature and concentration gradients in the fixed bed reactor play a major role in determining the product selectivity in highly oxidative conditions [21].

In this work, the specific selectivity towards CH_4 activation is investigated extending the scope to a series of simple metal oxide catalysts. The studied catalysts include rare-earth metal oxides (La_2O_3, Nd_2O_3, Y_2O_3), which are known for their activity in methane oxidation reactions [22], MgO, a model catalytic system for OCM investigation [4], and TiO_2, commonly employed as support material for its redox properties [23,24]. Unsteady-state operation experiments are performed by alternatively passing CH_4 and O_2 feeds to the catalytic bed at temperatures up to 900 °C, to evaluate the peculiar activity towards CH_4 activation and regenerating the active oxygen of the catalyst in the subsequent O_2 pulse. The transient evolution of products in the reactant pulses is analysed by means of fast FTIR spectroscopy (5 s temporal resolution) and mass spectrometry. The results reveal distinct selectivity of the different metal oxides at 900 °C towards partial oxidation of CH_4 to CO and H_2 and towards coupling of CH_4 to C_2H_6 and C_2H_4. Information on the extent of coke deposition was derived by analysis of the CO_x product evolved in the O_2 pulse. Insights into the participation of active lattice oxygen species are obtained and verified by thermogravimetric analysis of the catalysts.

2. Experimental section

2.1. Catalyst materials

La_2O_3 (99.99 %, Alfa Aesar), MgO (≥ 99 % trace metal basis, Sigma Aldrich), Nd_2O_3 (Nanografi, nanoparticles 25–40 nm, 99.95 %), TiO_2 (Alfa Aesar, rutile, 99.5 %) and Y_2O_3 (Aldrich, 99.99 %) were used as simple metal oxide catalysts without any further treatment.

2.2. Thermogravimetric analysis

Thermogravimetric analysis (TGA) of the samples was carried out in a METTLER TOLEDO SF/1100 thermogravimetric analyser by heating at a rate of 10 °C min^{-1} up to 1000 °C. The simple metal oxides samples were analysed under 100 mL min^{-1} flow of pure N_2 or diluted H_2 (5 vol % in N_2). No pretreatment of the catalyst samples was performed prior to TGA. Physical mixtures of 10 wt% carbon black (Vulcan XC 72 R) on simple metal oxides were prepared for TGA analysis in N_2.

2.3. Catalytic testing

200 mg of catalyst material (pelletised, crushed and sieved to the size range of 300–400 μm) was loaded into a quartz tubular reactor (6 mm OD, 4 mm ID), fixed between quartz wool layers. The temperature of the bed was monitored by a thermocouple inserted in the quartz wool in contact with the end of the catalytic bed. Gas feeds were controlled by a system of mass flow controllers (Bronkhorst) and two 4-way switching valves (VICI Valco) controlled by software. Each cycle of operation consists of alternation of diluted O_2 (25 vol% in He, 0–150 s), He flush (150–300 s) and CH_4 (300–450 s) feeds (50 mL min^{-1}) to the reactor. The data presented were obtained from the average of at least 3 cycles of operation, after a stable and reproducible composition of the effluent was achieved. The composition of the reactor effluent was analysed by combination of FTIR spectroscopy (ALPHA, Bruker) and mass spectrometry (Omnistar Pfeiffer Vacuum). At the reactor outlet, H_2 was detected using MS signal (m/z = 2). For the quantification of C_2H_6, calibration of the MS signal (m/z = 30) was performed at reaction conditions by gas chromatography injections taken at different moments of the CH_4 pulse performed across multiple stable cycles of operations.

3. Results and discussion

3.1. Thermogravimetric analysis

Thermogravimetric analysis is employed to characterise the catalyst samples and reveal the presence of active lattice oxygen species that can take part in the selective activation of methane. Three different experiments are conducted for each metal oxide catalyst. On the metal oxide samples, TGA is performed heating up the catalyst in N_2 atmosphere (blue lines) or in a reducing H_2 atmosphere (red lines) up to 1000 °C (Fig. 1). In H_2 atmosphere, a prominent decrease in the catalyst weight would be observed in correspondence with the abstraction of O species from the catalyst, at the temperatures at which the surface and bulk reduction processes are activated. In addition, a physical mixture of metal oxide and C black is prepared and tested for TGA in N_2 (black lines). In those conditions, an additional weight loss is introduced, corresponding to the gasification of the solid carbon operated by oxygen species which are thermally activated during the TGA heating ramp. By comparing the profiles obtained, the presence of active oxygen species in the catalysts lattice and their activity for both the oxidation of H_2 and gasification of C can be tested.

3.1.1. La_2O_3

Fig. 1A shows the TGA profiles obtained for La_2O_3. All the three TGA experiments showed similar weight loss profiles, with the highest extent observed for the N_2-TGA on the pure La_2O_3. In the case of C/La_2O_3, the smaller weight loss can be explained by the additional presence of solid C in the sample (10 wt% C on metal oxide), the significantly lower weight loss observed during the H_2-TGA indicates a possible instrumental limitation. To take into account the buoyancy effect, TGA of empty crucibles are conducted prior to each experiment and subtracted from the corresponding TGA profiles. An expansion of the La_2O_3 powders in the crucibles during TGA is detected, possibly connected with the cause of the discrepancy in the N_2 and H_2-TGA profiles. For the purpose of this investigation, however, qualitative information can be retrieved by the analysis of the first derivative of the weight loss profiles with respect to temperature, shown in Fig. 1B. The derivative profiles express the rate of weight change, and their minima characterise the temperatures at which weight loss processes reach their maximum rate. It is clear that two main weight loss phenomena take place on the La_2O_3 sample with a peak around 300 and 500 °C. At around 600 °C, an additional peak is detected in the derivative profiles, with the H_2-TGA profile showing a slightly lower temperature. Exposure of La_2O_3 to air at ambient conditions is known to promote bulk hydration and carbonation [25]. The important weight loss experienced by the La_2O_3 samples is independent from the gaseous atmosphere or the presence of C, suggesting that the phenomenon is associated with thermal decomposition of hydroxide and carbonate phases. Similar TGA profiles for La_2O_3 have been reported, although diverging decomposition temperatures are obtained on different samples [26,27]. In general, low temperature decomposition involves dehydration followed, at higher temperatures, by the decomposition of LaO(OH) and $La_2O_2CO_3$ species to La_2O_3.

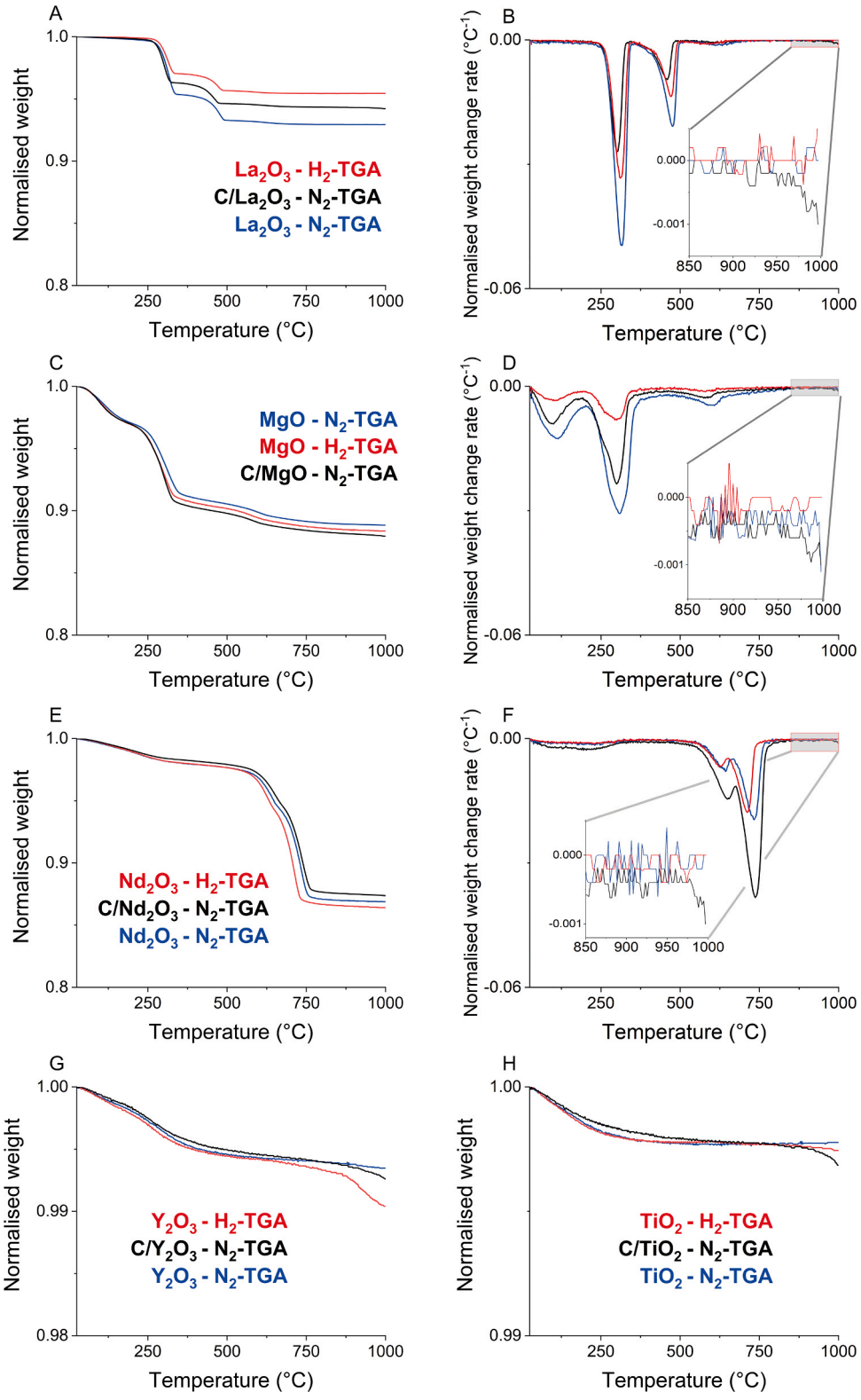

Fig. 1. Thermogravimetric analysis (TGA) of the different metal oxide catalysts (30–1000 °C, 10 °C min^{-1} heating rate) performed under N_2 (blue profiles), H_2 (red profiles). TGA profiles of C/metal oxide (C black 10 wt%) physical mixtures under N_2 (black profiles). Derivative of weight change is included for samples undergoing prominent weight losses. La_2O_3 (A-B), MgO (C-D), Nd_2O_3 (E-F), Y_2O_3 (G) and TiO_2 (H).

It has to be noted that decomposition of the La hydroxide and carbonate may hide the presence of additional less-significant weight loss processes. In particular, evolution of water and CO_2 could provoke the gasification of the C black employed for the N_2-TGA of the C/La_2O_3 sample. However, at temperatures higher than 600 °C, the TGA profile of C/La_2O_3 sample experiences a slow weight loss until it reaches a sudden acceleration approaching 1000 °C, as evidenced in the corresponding derivative profile. The singularity of this weight loss phenomenon, which is not observed in the C-free samples, reveals the presence of a limited amount of oxygen species which are able to

selectively activate C gasification.

3.1.2. MgO

Similar to the La_2O_3 case, three relevant weight loss processes occur for MgO (Fig. 1C) with derivative peaks at around 100, 300 and 580 °C (Fig. 1D). Evaporation of adsorbed water can take place during the first one, while the followings are explained by the decomposition of Mg hydroxides and carbonates which were formed upon prolonged air exposure at ambient conditions [28]. Contrarily to the La_2O_3 case, none of the three TGA profiles of MgO reaches a plateau. A small but continuous weight decrease is observed under all conditions at temperatures above 600 °C with a slight acceleration in the C/MgO sample at temperatures approaching 1000 °C, indicating contribution of C gasification processes. After the last intense weight loss at temperatures higher than ca. 900 °C, an additional weight loss process starts to be activated exclusively for the sample containing C black, indicating the presence of oxygen species active in C gasification at this temperature.

3.1.3. Nd_2O_3

The TGA profiles of Nd_2O_3 (Fig. 1E-F) show two pronounced weight loss steps with derivative peaks between 550 and 750 °C, assignable to the progressive dehydration and decarbonation of hydroxide and carbonate phases [29]. Also for this system, the derivative of weight change of the C/Nd_2O_3 sample shows a slight acceleration at temperatures close to 1000 °C, indicating activation of C gasification.

3.1.4. Y_2O_3, TiO_2

The TGA profiles of Y_2O_3 (Fig. 1G) and TiO_2 (Fig. 1H) do not show any relevant weight loss at low temperatures, implying that the samples are present in the form of pure oxides. The limited extent of weight change, below 1 % of the initial weight, resulted in noisy flat derivatives (not shown here). However, the absence of bulk phase decomposition processes increases the sensitivity of the technique regarding the discrimination of specific interaction of oxygen species with H_2 and solid C. At high temperatures, the profiles of H_2-TGA and N_2-TGA on the C-containing sample start to diverge from the N_2-TGA profile. The trends reveal an additional weight loss in presence of gaseous hydrogen or solid carbon, which identifies the participation of lattice oxygen in the oxidation of hydrogen and gasification of C, respectively.

In the case of Y_2O_3, the divergence of the TGA profiles start at around 650 °C and the weight loss is accentuated in the presence of H_2 atmosphere. This result demonstrates the presence of reducible oxygen species, seemingly confined at the surface of the catalyst, which can react with H_2 and, at higher temperatures, activate C gasification. Temperature programmed reduction studies confirmed the limited reducibility of Y_2O_3 support and the possibility of removing oxygen species from the lattice in highly reducing conditions [30].

Least weight loss (<0.05 wt%) was detected on the TiO_2 sample (Fig. 1H). Although TiO_2 is known for the excellent redox properties in photocatalytic application, it usually displays low reducibility in temperature programmed reduction experiments. Rutile TiO_2, in particular, shows very limited reducibility in H_2 and at higher temperatures compared to anatase TiO_2 [31]. At temperatures higher than 800 °C, an increased weight loss is noticed for the H_2-TGA profile and the N_2-TGA on the C-containing sample. Above this temperature, oxygen species of the TiO_2 lattice are active for the oxidation of H_2 and C. Contrarily to the case of Y_2O_3, the higher weight loss observed in presence of C black seems to suggest a preferential activity of oxygen species in TiO_2 towards the oxidation of solid C species.

3.1.5. Quantitative considerations

The thermogravimetric experiments indicated the availability of lattice O species for oxidation reactions involving H_2 and solid carbon species at high temperatures. The high sensitivity of TGA would permit the quantification of such O species. As discussed in the previous paragraph, concomitant phase decomposition processes must be considered, since they account for important weight losses especially in the low-mid temperature range. In order to perform a quantitative estimation of reactive lattice O species, we focused on the weight losses detected in the high temperature range (i.e. T > 800 °C), where major phase decomposition phenomena appear to be completed for all samples. In this temperature range (800–1000 °C), the weight losses detected in N_2-TGA are used as reference to account for residual phase decomposition phenomena. This considered, an estimation of the available reactive lattice O species can be made by comparing the weight losses experienced by the metal oxides during TGA under H_2 and N_2 flow (Table S1). Fig. 2 reports the weight losses experienced by the samples between 800 and 1000 °C, normalised to the molecular weight of the metal oxides. With the exception of La_2O_3 (*vide supra*), all the other samples exhibit a greater weight loss when exposed to H_2. This enhanced weight reduction, if assigned exclusively to lattice O species abstracted by H_2, can serve as a preliminary estimation of the amount of reactive lattice O species available in each sample (Fig. S1). In presence of C/metal oxide physical mixtures, a greater weight loss is experienced, deriving from the sum of the O and C loss from the sample. It is worth noticing that the ability to oxidise solid carbon differs substantially among the different metal oxide samples, suggesting a difference in reactivity of such lattice O species.

3.2. Catalytic activity – transient analysis of products

The catalytic activity tests were performed by exposing the catalyst bed to the alternation of gas feed atmospheres at different temperatures (300, 500, 700, 900 °C). The results presented are average of multiple stable cycles of operation, each cycle consisting of an oxidant pulse (0–150 s, 25 vol% O_2 in He), an inert flushing pulse (150–300 s, pure He) and a reducing pulse (300–450 s, pure CH_4), fed at constant flow rate (50 mL min^{-1}).

To observe the evolution of reaction products deriving from CH_4 activation, a minimum temperature of 700 °C was needed, indicating that the lattice oxygen is activated only above this temperature. Fig. 3 reports the profile of CO evolved in the CH_4 pulse (300–450 s) at 700 °C. Interestingly, CO was the only C product detected for the different simple metal oxide catalysts at 700 °C, accompanied by a slight increase in the H_2 signal (Fig. S2). To enhance the activation of CH_4 in the non-oxidative conditions of the catalytic test and clearly observe an evolution of C-containing products, higher temperatures are necessary (*vide infra*).

Above 700 °C, C_2 products are increasingly observed at higher temperatures. Fig. 4 reports the evolution of products for the different metal oxide catalysts during the CH_4 pulse (300–450 s) in the catalytic

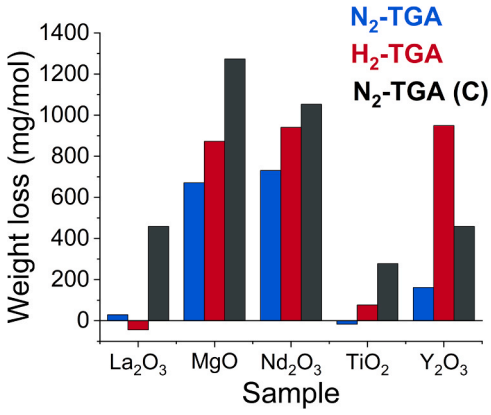

Fig. 2. Weight losses normalised over molecular weight of the oxides in the temperature range T = 800 – 1000 °C on the samples during N_2-TGA (blue profiles), H_2-TGA (red profiles) and N_2-TGA profiles of C/metal oxide physical mixtures (C black 10 wt%) (black profiles).

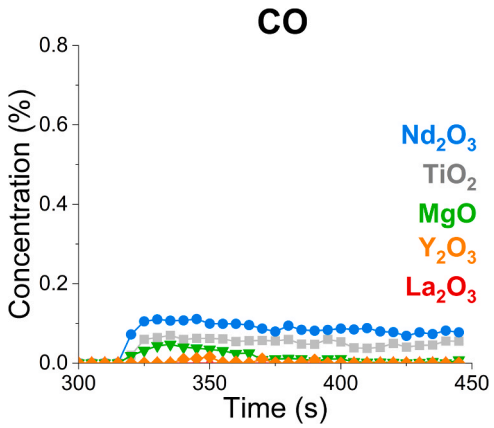

Fig. 3. Transient analysis of CO (FTIR) evolved during the CH_4 pulse (300–450 s) of the catalytic tests performed at 700 °C. The results are averaged over multiple stable cycles of operation. Results for Y_2O_3 (orange ◊), La_2O_3 (red ▲), Nd_2O_3 (blue ●), MgO (green ▼), TiO_2 (grey ■).

tests conducted at 900 °C. No CO_2 was produced in the reducing pulse for all the catalyst, excluding the promotion of total oxidation of CH_4 by the lattice oxygen of the simple metal oxides in absence of gaseous O_2.

3.2.1. Y_2O_3, La_2O_3

Y_2O_3 and La_2O_3 display similar catalytic behaviour, producing CO with high selectivity. The characteristic peak shape of the CO profile demonstrates the presence of reactive oxygen species in the oxides lattice, which undergo fast reaction with CH_4 at 900 °C until complete depletion. Those O species are restored in the subsequent O_2 pulse together with the activity of the catalyst. The signal of H_2 evolved in the CH_4 pulse well reproduces the CO trend, indicating that a mechanism of partial oxidation of methane is involved (Reaction 1, where $O_{(l)}$ stands for lattice oxygen).

$$CH_4 + O_{(l)} \quad = \quad 2H_2 \quad + CO \tag{1}$$

This oxygen is depleted in the interval of the reductive pulse of CH_4, indicating that it is possibly involving coordinatively unsaturated surface sites or oxygen species confined in the surface layers of the lattice. Ekstrom et al. [32] conducted isotopic studies of partial oxidation on rare earth metal oxides at 700 °C. They found that the isotopic composition of reaction products instantaneously followed the change in the isotopic composition of the methane feed. Presence of a small number of highly active sites was postulated, which are responsible for the instantaneous conversion of CH_4. The hypothesis was confirmed by the observation of rapid oxygen exchange between gas-phase and lattice oxygen atoms at 700 °C, which led to identify the active sites as oxygen atom in a vacancy site at the catalyst surface. In agreement with these results, Dixit et al. [33] observed H_2 and CO as main products during temperature programmed reduction of La_2O_3 in CH_4. By addition of gaseous oxygen, they noticed the increase in CH_4 conversion, with decrease in H_2 production and rise of CO_2 as main product. Those results reinforce the evidence of an intrinsic selectivity of the lattice oxygen in Y_2O_3 and La_2O_3 towards CH_4 partial oxidation (Reaction 1). Such selective behaviour is lost in presence of gaseous oxygen, where the extremely oxidative conditions promote exothermic reaction leading to total oxidation of CH_4 to CO_2 and H_2O.

Higher activity exhibited by Y_2O_3, corresponding to a larger amount of available oxygen species for CH_4 partial oxidation, can be explained as follows. A first naive consideration is on basis of the experimental conditions of the catalytic test, for which a fixed amount of catalyst was loaded into the reactor (0.2 g). Being Y a lighter element than La, a larger amount of oxygen is available in the Y_2O_3 catalytic bed. However, interpretation of the trends of the moles of CO produced with respect to the total oxygen available in the catalyst (Fig. S3) is not obvious.

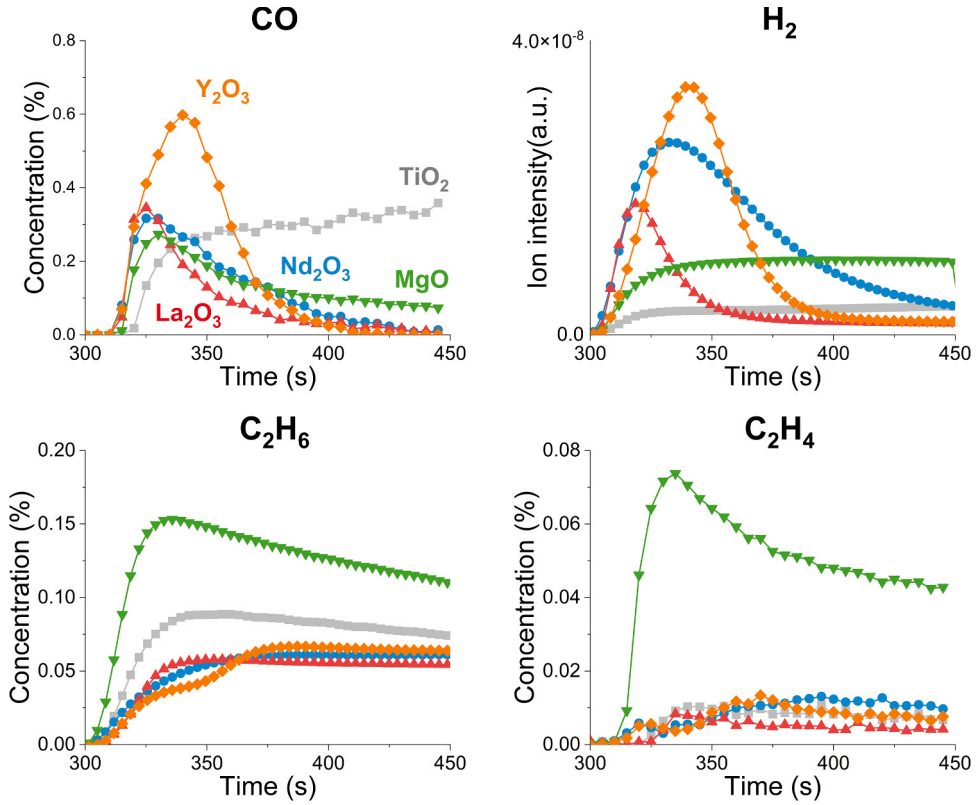

Fig. 4. Transient analysis of products (FTIR + MS) during the CH_4 pulse (300–450 s) of the catalytic tests performed at 900 °C. The results are averaged over multiple stable cycles of operation. Results for Y_2O_3 (orange ◊), La_2O_3 (red ▲), Nd_2O_3 (blue ●), MgO (green ▼), TiO_2 (grey ■).

Another factor is the lower surface oxygen vacancy formation energy of Y_2O_3 compared to La_2O_3, which can explain the higher availability of reactive oxygen species and the better performance in CH_4 partial oxidation [34]. This consideration is in agreement with the results obtained from TGA, which showed enhanced reducibility of Y_2O_3 (Fig. 1G) in presence of H_2 and C at high temperatures. Poor activity towards C_2 product is observed for both Y_2O_3 and La_2O_3, with C_2H_6 detected as the main C_2 product. Although La_2O_3 is an active catalytic system for OCM, its activity towards C_2 species in the non-oxidative conditions of the CH_4 pulse is minimal. In the case of Y_2O_3, both profiles of C_2H_6 and C_2H_4 experience a rise after 350 s. This time fits well with the moment of the drop of the CO and H_2 signals and seems related to the depletion of the active oxygen species in the catalyst. The scarcity of highly active oxygen species can prevent the oxidation of the CH_x intermediates to CO, favour non-oxidative processes for the decomposition of methane and resulting in an increased formation of C_2 species.

3.2.2. Nd_2O_3

When tested for catalytic oxidation of CH_4, rare-earth metal oxides generally exhibit similar products distribution and selectivity trends [10]. Evidence of isotopic exchange of oxygen on rare-earth metal oxides revealed a high lattice oxygen mobility. The active participation of lattice oxygen in oxidation reactions was confirmed by the similar activation energy found for both $^{18}O_2$-exchange and H_2 oxidation processes [22]. Thus, it is not surprising to find high partial oxidation activity also for Nd_2O_3 (Fig. 4), in agreement with the behaviour exhibited by Y_2O_3 and La_2O_3. However, differences are noticed in particular regarding the formation of H_2, whose signal is surprisingly high for Nd_2O_3 and decays more slowly than the corresponding CO signal. Although the literature on the activity of pure Nd_2O_3 is scarce, addition of Nd as catalytic promoter for the conversion of CH_4 is reported to enhance the activity towards partial oxidation products and especially H_2 selectivity at high temperatures [35,36]. Moreover, among a series of lanthanides, Campbell et al. [9] reported the highest activity in the oxidative coupling of methane on Nd_2O_3.

In absence of gaseous oxygen, a reaction route responsible for the surplus of H_2 can be identified in the catalytic decomposition of CH_4 (Reaction 2), which proceeds through progressive dehydrogenation steps (Reaction 2a) until solid carbon ($C_{(ads)}$) is deposited on the surface of the catalyst and H_2 released from the surface (Reaction 2b). The analysis of the C deposition extent can be performed on the basis of the CO_x species evolved during the O_2 pulse of the unsteady-state experiment (Fig. 5). The formation of CO_x species over Nd_2O_3 is substantially higher than over Y_2O_3 and La_2O_3, indicating the presence of carbon deposits in larger amount. Thus, Nd_2O_3 proves to be highly active for the decomposition of CH_4. From these results, it can be concluded that partial oxidation products are readily formed at the beginning of the CH_4 pulse, when there is abundance of surface oxygen species. After depletion of this active oxygen, methane decomposition is more prominently activated on Nd_2O_3 and proceeds by stepwise dehydrogenation steps leading to accumulation of solid C and release of H_2.

$$CH_4 = C_{(ads)} + 2H_2 \quad (2)$$

$$CH_x = CH_{x-1(ads)} + H_{(ads)} \quad (2a)$$

$$2H_{(ads)} = H_2 \quad (2b)$$

The enhanced activity in CH_4 decomposition is not directly associated with general increase in the production of C_2 species. The profiles of C_2 species (Fig. 4) visibly indicates that the ratio of C_2H_4 to C_2H_6 is higher in the case of Nd_2O_3, confirming an intrinsic catalytic activity towards dehydrogenation reactions. However, such predisposition towards dehydrogenation reactions ultimately favours the formation of solid C and H_2 products rather than intermediates C_2 species.

3.2.3. MgO

MgO shows a unique intrinsic activity for the selective conversion of CH_4 to C_2 species (Fig. 4). Lattice O species are available, as confirmed by the continuous release of CO. The CO release rises slowly at the beginning of the CH_4 pulse, without a pronounced peaked profile. The signal then progressively decays, maintaining an almost constant release of CO until the end of the pulse. Peil et al. [37] demonstrated the availability of surface reactive oxygen species in the non-reducible MgO via steady state isotopic transient kinetic analysis (SSITKA). They also reported the increased mobility of MgO lattice oxygen species with temperature, which suggests their increased availability to oxidation reactions such as the conversion of CH_4 to CO_x species. $^{18}O/^{16}O$ isotopic transient kinetics experiments on MgO revealed oxygen exchange with the first surface layers of the catalyst activated at around 600 °C. The evidence of direct participation of lattice O species in the conversion of CH_4 to CO indicates that, even in non-reducible metal oxides as MgO, some highly reactive O species are available at the surface and their participation to the reaction mechanism for high temperature oxidation reactions, as methane partial oxidation and oxidative coupling, must be considered.

The activity of MgO in OCM has driven the researchers' attention to the individuation of active sites for the initial CH_4 activation step, namely the formation of a methyl radical ($\bullet CH_3$) by H abstraction (Reaction 3). Highly basic O sites as peroxide (O_2^{2-}) and superoxide (O_2^-) species have been pointed out as responsible for the initial step of the CH_4 activation both by experimental works and ab initio molecular dynamics [38,39].

$$CH_4 + O^{2-} = \bullet CH_{3(g)} + OH^-_{(ads)} \quad (3)$$

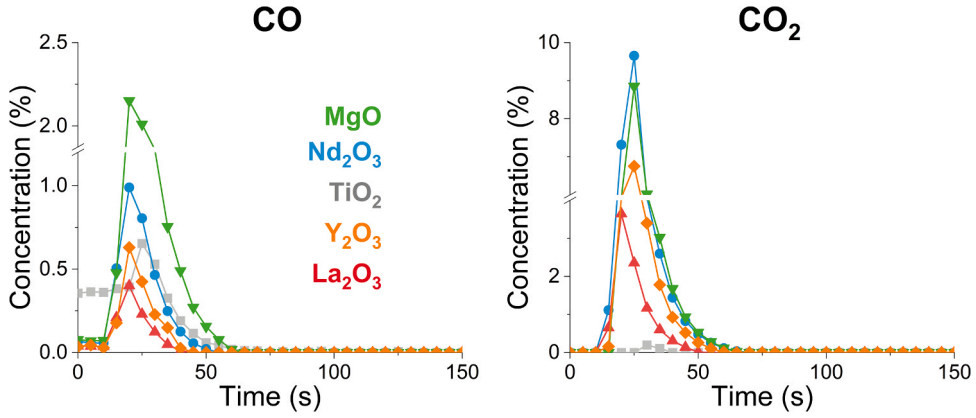

Fig. 5. Transient analysis of CO_x products (FTIR) evolved during the O_2 pulse (300–450 s, 25 vol% O_2 in He) of the catalytic tests performed at 900 °C. The results are averaged over multiple stable cycles of operation. Results for Y_2O_3 (orange ◊), La_2O_3 (red ▲), Nd_2O_3 (blue ●), MgO (green ▼), TiO_2 (grey ■).

The release of methyl radicals to the gas phase is condition to the formation of coupling products (i.e. C_2H_6 and C_2H_4). A simultaneous parallel path involving the trapping of the methyl radical on the surface to form methoxy intermediates (Reaction 4) is considered as the source of a complex network of reactions leading to CO_x formation (Reaction 5) [40].

$$\bullet CH_{3(g)} + O^{2-} = CH_3O^-_{(ads)} \quad (4)$$

$$CH_3O^-_{(ads)} = CO + H_2 + e^- \quad (5)$$

Contrary to what has been shown for rare earth metal oxides, the profiles of CO and H_2 do not match for MgO (Fig. 4). The H_2 signal does not present any peak and, after the initial rise, maintains a constant value for all the duration of the CH_4 pulse. The oxygen species responsible for CO formation are not completely depleted in an initial fast process to partially oxidise CH_4 but rather continuously supplied. Considering the constant value of H_2, it appears that MgO can continuously activate the decomposition of the CH_4 molecules to C and H_2. While the H_2 is instantaneously released, the C deposits are oxidised to CO by the lattice oxygen at a slower rate. Such mechanism would favour the accumulation of carbon deposits.

The slow rate of methane partial oxidation promoted by the lattice oxygen can also explain the high selectivity observed for C_2 products. Instead of rapidly converting CH_4 to CO by means of active surface oxygen species, $\bullet CH_3$ radicals are formed on MgO and allowed to couple in the gas phase to form C_2H_6 (Reaction 6) without undergoing further oxidation steps [41,42]. The activity towards the dehydrogenation of methane is reflected also in high activity towards selective dehydrogenation of C_2H_6 to C_2H_4 (Reaction 7), which is detected in exceptionally high concentration among the metal oxides screened.

$$2CH_4 = C_2H_6 + H_2 \quad (6)$$

$$C_2H_6 = C_2H_4 + H_2 \quad (7)$$

The dehydrogenation of C_2H_6 to C_2H_4 also contributes to an additional release of H_2, which can explain its constant signal detected along the whole CH_4 pulse.

3.2.4. TiO_2

The highly redox properties of TiO_2 (rutile) are clearly observed in the catalytic CH_4 activation (Fig. 4). At 900 °C, a constant formation of CO is detected, which proceeds until the end of the CH_4 pulse. Towards the end of the reductive CH_4 pulse, the concentration of CO is extremely high compared to the other mixed oxides, indicating a constant supply of oxygen species from the catalyst lattice. Although the profiles of CO and H_2 match in shape, the release of H_2 is substantially lower when compared with the other simple oxides investigated. This observation suggests poor activity towards dehydrogenation reactions for TiO_2. It is possible that H atoms abstracted from the CH_4 molecules adsorb in the form of surface hydroxyl groups and promote the release of water [43]. Due to the presence of a water condenser at the reactor outlet, no information about the amount of water release could be derived from the present data. On the other hand, a significant release of C_2H_6 is noticed, which is found higher than the Y_2O_3, La_2O_3 and Nd_2O_3 cases. Very low selectivity towards C_2H_4 further indicates a poor activity towards dehydrogenation reactions. The remarkably low release of CO_x species during the O_2 pulse (Fig. 5) indicates that accumulation of carbon deposits on TiO_2 is prevented by the high availability of reactive lattice oxygen species.

Due to the long-lasting release of active lattice oxygen observed for MgO and TiO_2, a similar catalytic experiment with an extended CH_4 pulse duration (900 s) was performed. The results (Fig. S4) confirm the selectivity trends observed with the short reducing pulse, with preferential generation of CO on TiO_2 and C_2 products on MgO. In terms of coking, the exposure of the catalysts to a longer CH_4 pulse is expected to favour the accumulation of carbon deposits on the catalyst surface, resulting in a larger release of CO_x products in the oxidant pulse. The CO and CO_2 profiles obtained during the O_2 pulse (Fig. 6) show that the amounts of CO and CO_2 released on the MgO catalyst drastically increase compared to the short CH_4 pulse case (Fig. 5). The ability of MgO to activate CH_4 and promote dehydrogenation, together with the absence of reactive oxygen species for its oxidation to CO, favour the accumulation of carbon deposits, and the release of C_2 species. For the TiO_2 catalyst, in contrast, the release of CO_x species in the O_2 pulse is limited. The high availability of lattice oxygen for the oxidation of CH_4 prevented the accumulation of solid carbon by directly promoting its selective oxidation to CO. Interestingly, the residual carbon deposits removed in O_2 are selectively gasified to CO, with very limited CO_2 formation. This peculiar selectivity of TiO_2 towards the oxidation of solid carbon deposits makes it an interesting support for the design of catalysts for selective CH_4 conversion.

4. Conclusions

The intrinsic activity of simple metal oxides towards CH_4 activation has been evaluated by unsteady-state operation catalysis and transient analysis of the product stream. In unsteady-state conditions, i.e. CH_4 and O_2 alternatively fed to the reactor, temperatures higher than 700 °C are necessary to activate the catalytic conversion of CH_4. A specific reactive lattice oxygen species activates partial oxidation of CH_4 to CO and H_2 with high selectivity in rare-earth metal oxides (Y_2O_3, La_2O_3 and Nd_2O_3) at 900 °C. Among these, Nd_2O_3 exhibits high activity in decomposition of CH_4 that contributes to additional H_2 formation and enhanced formation of solid C. The best performance in terms of C_2 coupling products is found for the MgO catalyst, on which less pronounced reactivity of lattice oxygen species allows continuous C_2H_6 and C_2H_4 formation without undergoing further oxidation steps. On the other hand, the high redox properties of TiO_2 intervene in the CH_4 oxidation by selectively oxidising it to CO. A constant supply of active O from TiO_2 lattice is detected, which makes the system an ideal support to prevent accumulation of carbon deposits in CH_4 conversion reactions. Thermogravimetric analysis of the simple metal oxides in H_2 and in presence of solid C confirmed the direct participation of lattice oxygen in the oxidation reactions at high temperature.

The results here presented clarify the specific role of simple metal oxides in the activation of CH_4, which appears closely related to the nature of their surface oxygen species. It is suggested that, in oxidative conditions, the development of highly exothermic reaction routes, promoted by the presence of molecular oxygen, can enhance the rate of unselective total oxidation paths and ultimately control the distribution of products.

Funding

Financial support by Japan Science and Technology agency (JST) through the PRESTO program (No. JPMJPR16S3) is greatly acknowledged.

CRediT authorship contribution statement

Pinto Donato: Writing – review & editing, Writing – original draft, Visualization, Validation, Methodology, Investigation, Data curation, Conceptualization. **Urakawa Atsushi:** Writing – review & editing, Supervision, Resources, Project administration, Methodology, Investigation, Funding acquisition, Conceptualization.

Declaration of Competing Interest

The authors declare the following financial interests/personal relationships which may be considered as potential competing interests: Atsushi Urakawa reports financial support was provided by Japan

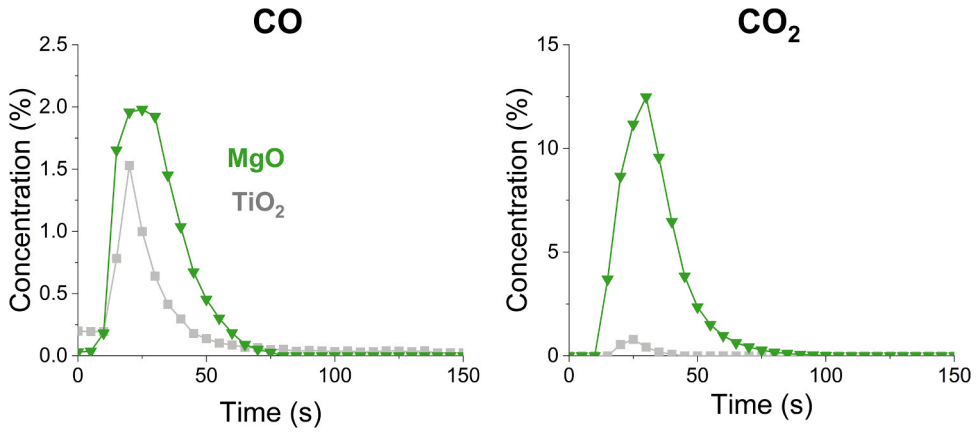

Fig. 6. Transient analysis of CO_x products (FTIR) evolved during the O_2 pulse (0–150 s, 25 vol% O_2 in He) of the catalytic tests performed at 900 °C with extended CH_4 pulse duration (900 s). The results are averaged over multiple stable cycles of operation. Results for MgO (green ▼) and TiO_2 (grey ■).

Science and Technology Agency. If there are other authors, they declare that they have no known competing financial interests or personal relationships that could have appeared to influence the work reported in this paper

Appendix A. Supporting information

Supplementary data associated with this article can be found in the online version at doi:10.1016/j.cattod.2025.115337.

Data availability

Data will be made available on request.

References

[1] K. Aasberg-Petersen, I. Dybkjær, C.V. Ovesen, N.C. Schjødt, J. Sehested, S. G. Thomsen, Natural gas to synthesis gas – catalysts and catalytic processes, J. Nat. Gas. Sci. Eng. 3 (2011) 423–459.
[2] C. Hammond, S. Conrad, I. Hermans, Oxidative methane upgrading, ChemSusChem 5 (2012) 1668–1686.
[3] A.A. Latimer, A. Kakekhani, A.R. Kulkarni, J.K. Nørskov, Direct methane to methanol: the selectivity–conversion limit and design strategies, ACS Catal. 8 (2018) 6894–6907.
[4] P. Schwach, X. Pan, X. Bao, Direct conversion of methane to value-added chemicals over heterogeneous catalysts: challenges and prospects, Chem. Rev. 117 (2017) 8497–8520.
[5] T.V. Choudhary, E. Aksoylu, D.Wayne Goodman, Nonoxidative activation of methane, Catal. Rev. 45 (2003) 151–203.
[6] C. Li, G. Li, Q. Xin, FT-IR spectroscopic studies of methane adsorption on magnesium oxide, J. Phys. Chem. 98 (1994) 1933–1938.
[7] G.E. Keller, M.M. Bhasin, Synthesis of ethylene via oxidative coupling of methane: I. Determination of active catalysts, J. Catal. 73 (1982) 9–19.
[8] J.M. DeBoy, R.F. Hicks, The oxidative coupling of methane over alkali, alkaline earth, and rare earth oxides, Ind. Eng. Chem. Res. 27 (1988) 1577–1582.
[9] K.D. Campbell, H. Zhang, J.H. Lunsford, Methane activation by the lanthanide oxides, J. Phys. Chem. 92 (1988) 750–753.
[10] K. Otsuka, K. Jinno, A. Morikawa, Active and selective catalysts for the synthesis of C_2H_4 and C_2H_6 via oxidative coupling of methane, J. Catal. 100 (1986) 353–359.
[11] S. Sato, R. Takahashi, M. Kobune, H. Gotoh, Basic properties of rare earth oxides, Appl. Catal. A Gen. 356 (2009) 57–63.
[12] Y.S. Su, J.Y. Ying, W.H. Green, Upper bound on the yield for oxidative coupling of methane, J. Catal. 218 (2003) 321–333.
[13] T. S.B.F. Da Ros, M. Schwaab, N.J. Castro de Jesus, J.C. Pinto, Oxidative coupling of methane for ethylene production: reviewing kinetic modelling approaches, thermodynamics and catalysts, Processes 9 (2021) 2196.
[14] A. Obradović, J.W. Thybaut, G.B. Marin, Oxidative coupling of methane: opportunities for microkinetic model-assisted process implementations, Chem. Eng. Technol. 39 (2016) 1996–2010.
[15] L. Hu, D. Pinto, A. Urakawa, Active reactions and spatial gradients in oxidative coupling of methane, Catalysis, R. Soc. Chem. 32 (2020) 203–223.
[16] K. Takanabe, E. Iglesia, Rate and selectivity enhancements mediated by OH Radicals in the Oxidative Coupling of Methane Catalyzed by $Mn/Na_2WO_4/SiO_2$, Angew. Chem. Int. Ed. 47 (2008) 7689–7693.
[17] X. Zhou, Y. Pang, Z. Liu, E.I. Vovk, A.P. van Bavel, S. Li, Y. Yang, Active oxygen center in oxidative coupling of methane on La_2O_3 catalyst, J. Energ. Chem. 60 (2021) 649–659.
[18] X.P. Dai, R.J. Li, C.C. Yu, Z.P. Hao, Unsteady-state direct partial oxidation of methane to synthesis gas in a fixed-bed reactor using $AFeO_3$ (A = La, Nd, Eu) perovskite-type oxides as oxygen storage, J. Phys. Chem. B 110 (2006) 22525–22531.
[19] K.P. Peil, J.G. Goodwin, G. Marcelin, Steady-state vs non-steady-state transient kinetic analysis of surface coverages during the oxidative coupling of methane, J. Catal. 132 (1991) 556–559.
[20] R. Spinicci, Oxidative coupling of methane as studied by temperature programmed reaction and transient response methods, Catal. Today 4 (1989) 311–322.
[21] L. Hu, D. Pinto, A. Urakawa, Catalytic oxidative coupling of methane: heterogeneous or homogeneous reaction? ACS Sustain. Chem. Eng. 11 (2023) 10835–10844.
[22] M.P. Rosynek, Catalytic properties of rare earth oxides, Catal. Rev. 16 (1977) 111–154.
[23] M. Kotobuki, R. Leppelt, D.A. Hansgen, D. Widmann, R.J. Behm, Reactive oxygen on a Au/TiO_2 supported catalyst, J. Catal. 264 (2009) 67–76.
[24] Q.G. Yan, W.Z. Weng, H.L. Wan, H. Toghiani, R.K. Toghiani, C.U. Pittman, Activation of methane to syngas over a Ni/TiO_2 catalyst, Appl. Catal. A Gen. 239 (2003) 43–58.
[25] P. Fleming, R.A. Farrell, J.D. Holmes, M.A. Morris, The rapid formation of $La(OH)_3$ from La_2O_3 powders on exposureto water vapor, J. Am. Ceram. Soc. 93 (2010) 1187–1194.
[26] S. Bernal, F.J. Botana, R. García, J.M. Rodríguez-Izquierdo, Thermal evolution of a sample of La_2O_3 exposed to the atmosphere, Thermochim. Acta 66 (1983) 139–145.
[27] Q. Mu, Y. Wang, Synthesis, characterization, shape-preserved transformation, and optical properties of $La(OH)_3$, $La_2O_2CO_3$, and La_2O_3 nanorods, J. Alloy. Compd. 509 (2011) 396–401.
[28] N. Khan, D. Dollimore, K. Alexander, F.W. Wilburn, The origin of the exothermic peak in the thermal decomposition of basic magnesium carbonate, Thermochim. Acta 367-368 (2001) 321–333.
[29] L.De Almeida, S. Grandjean, N. Vigier, F. Patisson, Insights into the thermal decomposition of Lanthanide(III) and Actinide(III) oxalates – from Neodymium and cerium to Plutonium, Eur. J. Inorg. Chem. 2012 (2012) 4986–4999.
[30] H. Liu, H. Wu, D. He, Methane conversion to syngas over Ni/Y_2O_3 catalysts — Effects of calcination temperatures of Y_2O_3 on physicochemical properties and catalytic performance, Fuel Process. Technol. 119 (2014) 81–86.
[31] J. Li, G. Lu, G. Wu, D. Mao, Y. Guo, Y. Wang, Y. Guo, Effect of TiO_2 crystal structure on the catalytic performance of Co_3O_4/TiO_2 catalyst for low-temperature CO oxidation, Catal. Sci. Technol. 4 (2014) 1268–1275.
[32] A. Ekstrom, J.A. Lapszewicz, A study of the mechanism of the partial oxidation of methane over rare earth oxide catalysts using isotope transient techniques, J. Phys. Chem. 93 (1989) 5230–5237.
[33] M. Dixit, A. Menon, R. Baruah, A. Bhargav, S. Sharma, Oxidative activation of methane on lanthanum oxide and nickel-lanthanum oxide catalysts, React. Kinet. Mech. Catal. 115 (2015) 611–624.
[34] Y. Hinuma, T. Toyao, T. Kamachi, Z. Maeno, S. Takakusagi, S. Furukawa, I. Takigawa, K.-i Shimizu, Density functional theory calculations of oxygen vacancy formation and subsequent molecular adsorption on oxide surfaces, J. Phys. Chem. C 122 (2018) 29435–29444.
[35] M. Caballero, G. Del Angel, A. Bonilla-Sánchez, I. Rangel-Vázquez, A. Arrieta, A. Vázquez-Zavala, L. Huerta, M. Salgado, High selectivity to hydrogen on the methane decomposition over $Rh/\gamma\text{-}Al_2O_3$–Nd_2O_3 catalysts, Int. J. Hydrog. Energy 41 (2016) 23247–23259.
[36] V.R. Choudhary, K.C. Mondal, A.S. Mamman, U.A. Joshi, Carbon-free dry reforming of methane to syngas over $NdCoO_3$ perovskite-type mixed metal oxide catalyst, Catal. Lett. 100 (2005) 271.

[37] K.P. Peil, G. Marcelin, J.G. Goodwin, The role of lattice oxygen in the oxidative coupling of methane, in: E.E. Wolf (Ed.), Methane Conversion by Oxidative Processes: Fundamental and Engineering Aspects, Springer Netherlands, Dordrecht, 1992, pp. 138–167.
[38] D. Cordischi, V. Indovina, M. Occhiuzzi, Thermal stability and chemical reactivity of $(O_2^-)_s$ species adsorbed on MgO surfaces, J. Chem. Soc. Faraday Trans. I 74 (1978) 456–465.
[39] A. Ishikawa, Y. Tateyama, What is the active site for the oxidative coupling of methane catalyzed by MgO? A metadynamics-biased ab initio molecular dynamics study, J. Phys. Chem. C 124 (2020) 6054–6062.
[40] M. Anpo, G. Costentin, E. Giamello, H. Lauron-Pernot, Z. Sojka, Characterisation and reactivity of oxygen species at the surface of metal oxides, J. Catal. 393 (2021) 259–280.
[41] D.J. Driscoll, W. Martir, J.X. Wang, J.H. Lunsford, Formation of gas-phase methyl radicals over magnesium oxide, J. Am. Chem. Soc. 107 (1985) 58–63.
[42] R. Schlögl, Heterogeneous Catalysis, Angew. Chem. Int. Ed. 54 (2015) 3465–3520.
[43] S. Huygh, A. Bogaerts, K.M. Bal, E.C. Neyts, High coke resistance of a TiO_2 Anatase (001) catalyst surface during dry reforming of methane, J. Phys. Chem. C 122 (2018) 9389–9396.